

Journal of Materials Chemistry C

Accepted Manuscript



This is an *Accepted Manuscript*, which has been through the Royal Society of Chemistry peer review process and has been accepted for publication.

Accepted Manuscripts are published online shortly after acceptance, before technical editing, formatting and proof reading. Using this free service, authors can make their results available to the community, in citable form, before we publish the edited article. We will replace this *Accepted Manuscript* with the edited and formatted *Advance Article* as soon as it is available.

You can find more information about *Accepted Manuscripts* in the [Information for Authors](#).

Please note that technical editing may introduce minor changes to the text and/or graphics, which may alter content. The journal's standard [Terms & Conditions](#) and the [Ethical guidelines](#) still apply. In no event shall the Royal Society of Chemistry be held responsible for any errors or omissions in this *Accepted Manuscript* or any consequences arising from the use of any information it contains.

The First Aggregation-Induced Emission Fluorophore as a Solution Processed Host Material in Hybrid White Organic Light-Emitting Diodes

Received 00th January 20xx,
Accepted 00th January 20xx

DOI: 10.1039/x0xx00000x

www.rsc.org/

Yi-Ting Lee,^a Yung-Ting Chang,^b Chao-Tsen Chen*^a and Chin-Ti Chen*^b

A judicious structure design of bis(3,5-di(9*H*-carbazol-9-yl)phenyl)amine (CzPA) and 1,1,2,2-tetraphenylethene (TPE) hybrid generates the first aggregation-induced emission (AIE) fluorophore, **CzPATPE**, as a solution processed host material in hybrid white organic light-emitting diode (OLED). Small molecule **CzPATPE** has been verified for the amorphous characteristics by a featureless halo in powder X-ray diffraction spectra and a glass transition temperature as high as 180 °C. Fluorescence images indicate that a homogenous thin film of **CzPATPE** is obtained from a solution drop-casting process. Solution (THF/water) fluorescence spectroscopy study clearly demonstrates a typical AIE property of **CzPATPE**. Whereas **CzPATPE** is virtually non-emissive in common organic solvents, thin film photoluminescence (PL) spectroscopy shows that **CzPATPE** has a strong sky blue emission around 495 nm with a relatively wide full width at half maximum (FWHM) about 95 nm and a reasonable PL quantum yield of 40%. Low temperature time-gated PL spectroscopy identifies **CzPATPE**'s triplet optical gap energy $E_T \sim 2.05\text{--}2.16$ eV, which is barely enough for phosphorescence dopant, tris(2-phenylquinoline) iridium (III) (Ir(2-phq)₃) ($E_T \sim 2.13$ eV). **CzPATPE** is solution processable to be a sky blue emissive host material for orange dopant in the hybrid white OLED, ITO/PEDOT:PSS (65 nm)/**CzPATPE**:Ir(2-phq)₃(99.9:0.1, ~40 nm)/TmPyPB(50 nm)/CsF (2 nm)/Al(100 nm). This AIE hybrid white OLED displays white electroluminescence (EL) with colour chromaticity of CIE_{x,y}(0.36, 0.43). Although the maximum EL efficiency is modest 3.4 cd/A or 1.8 lm/W, the white OLED has a colour rendering index (CRI) of 72, which is unusually high considering the orange dopant and two-colour white feature. We attribute such CRI to the relatively large FWHM of **CzPATPE**.

Introduction

In order to achieve high electroluminescence (EL) efficiency and high colour rendering index (CRI), the common configuration of high performance white organic light-emitting diodes (WOLEDs) involves multiple phosphorescent dopants which are separated by host material in a multiple layer construction.¹ However, the fabrication process of such WOLEDs is complicate and expensive. Recently, the hybrid of blue fluorescence host and single phosphorescence dopant (either yellow or orange) has attracted much attention in WOLEDs in the light of materials stability (blue phosphorescent dopant is particularly not stable) and the simplicity of device structure or fabrication.² The solution process instead of vacuum-thermal deposition process is better or more attractive in terms of cost, time, and the panel size of OLED fabrication.³ Materials wise, small molecular materials are superior to polymeric materials because of easy synthesis and practical purification. However, small molecular materials are prone to crystallization or aggregation in thin film state because of low glass transition temperature (T_g).⁴ Thus, useful host material (of phosphorescent dopant) suitable for solution process should be high in T_g , triplet

energy gap (E_T), and solid state fluorescence quantum yield (ϕ_f). More ideally, fluorescent blue emission of such host material used in hybrid WOLEDs should have a wide emission band width in order to compensate the loss of CRI due to the single phosphorescent dopant involved in the simplified device fabrication.

Most organic luminogens are non-emissive or weakly emissive in high concentration solution or in solid state like neat thin film because of aggregation-caused quenching (ACQ) behavior.⁵ In 2001, Tang's group proposed a novel phenomenon of aggregation-induced emission (AIE), of which the intensity is very weak in solution but it intensifies as aggregates are formed.⁶ Chemical moiety tetraphenylethene (TPE) is one of the iconic units for outstanding AIE and facile synthesis.⁷ By incorporating TPE unit onto bis(3,5-di(9*H*-carbazol-9-yl)phenyl)amine (**CzPA**), a potent moiety for amorphous morphology and high E_T ,⁸ we have successfully synthesized and demonstrated that the first AIE fluorophore **CzPATPE** (Scheme 1) as a solution processed host material for hybrid WOLEDs. Very recently, a deep blue AIEgen, 3TPA-CN,⁹ was shown to be an efficient host material for a phosphorescence dopant in vacuum-thermal fabricated orange OLEDs.

Scheme 1 Synthesis of CzPATPE.

Results and discussion

^a Department of Chemistry, National Taiwan University, Taipei 10617, Taiwan.

^b Institute of Chemistry, Academia Sinica, Taipei 11529, Taiwan. *Email: chintchen@gate.sinica.edu.tw; Fax: +886 2 27831237; Tel: + 886 2 27898542

† Electronic Supplementary information (ESI) available: ¹H, ¹³C NMR and HR-MALDI-TOF Mass spectra. See DOI: 10.1039/x0xx00000x

3,5-di(9*H*-carbazol-9-yl)-*N*-(3,5-di(9*H*-carbazol-9-yl)-phenyl)-*N*-(4-(1,2,2-triphenylvinyl)phenyl)aniline **CzPATPE** was efficiently synthesized in three steps (Scheme 1). Precursors 4-(1,2,2-triphenylvinyl)aniline (TPENH₂) and 9,9'-(5-bromo-1,3-phenylene)bis(9*H*-carbazole) (BrmCP) were synthesized by known literature procedures.^{10,11} **CzPATPE** was readily obtained by the Pd-catalysed amination of BrmCP with TPENH₂.

Solid state **CzPATPE** exhibits amorphous or semi-amorphous feature as indicated in DSC thermograms (Figure 1a) and X-ray diffraction spectra of solution drop-casting thin film on a silicon wafer (Figure 1b). The host material shows relatively high T_g s at 181 °C, which is clearly shown in all repeating scans. Furthermore, crystallization temperature (T_c) of **CzPATPE** can be identified as the

exothermic signal peaked at 229 °C, which is relatively broad and dull, indicating the weak tendency of crystallization. However, a strong endothermic signal of melting temperature (T_m) was detected at 329 °C in the first heating scan. X-ray diffraction spectra of the solution drop-casting thin film basically display a featureless broad halo, indicative of the amorphous nature of **CzPATPE** thin films. Such amorphous nature has been further verified in the AIE study of a solution (dichlorobenzene) drop-casting thin film, which is homogenous vision wise (Fig. 2).

Fig. 1 (a) DSC thermograms. (b) X-ray diffraction spectra of **CzPATPE** thin film on a substrate of silicon wafer.

Fig. 2 **CzPATPE** drop-casting solution under visible light (far left) and under UV illumination during the solvent evaporation at ~90 °C (the rest of six photographs).

Regarding thermal stability, **CzPATPE** was studied by thermogravimetric analysis (TGA). TGA was conducted under a nitrogen atmosphere with a heating rate of 20 °C min⁻¹. Figure 3 illustrates the thermal decomposition temperature of **CzPATPE**, which is as high as 543 °C (5% weight loss).

Fig. 3 TGA thermogram of **CzPATPE**.

In further experimental demonstration of AIE, THF and water were chosen as the solvent pair for its good miscibility. As shown clearly in Fig. 4a, THF solution of **CzPATPE** is virtually non-emissive. Fluorescence became discernible (peaked around 500 nm) when the water volume fraction (f_w) of **CzPATPE** THF solution is beyond 20%, where the precipitates of **CzPATPE** take place in solution. Such solution fluorescence characteristics are very typical for other AIEgens.

Fig. 4 **CzPATPE** THF solution with various water volume fraction (f_w): (a) Fluorescence image. (b) Fluorescence spectra (c) Variation of fluorescence intensity and fluorescence wavelength ($\lambda_{\max}^{\text{fl}}$).

Regarding fluorescence wavelength ($\lambda_{\max}^{\text{fl}}$), **CzPATPE** THF/water solution exhibits progressively blue-shifting emission, 503, 501, 493 nm, when the water fraction is increased from 20, 60 to 90%, respectively (Fig. 4b and 4c). Solution drop-casting thin film of **CzPATPE**, which is mainly in amorphous state, has a $\lambda_{\max}^{\text{fl}}$ around 495 nm. Blue-shifted emission wavelength is commonly observed for many TPE-containing AIE materials.^{9,12} This has been attributed to the change in the packing order of the aggregates from an amorphous state to a crystalline one.^{12c} On the other hand, the full width at half maximum (FWHM) of **CzPATPE** fluorescence spectrum is quite large ~95 nm, which is a common feature of TPE-based AIE fluorophores. A large FWHM is beneficial for achieving white CIE_{x,y} chromaticity and high CRI of WOLEDs. By using integrating-sphere method,¹³ fluorescence quantum yield (ϕ_f) of **CzPATPE** in solid state

(thin film) was determined to be ~40%, which suffices its usage in hybrid WOLEDs.

For orange phosphorescence dopant tris(2-phenylquinoline) iridium (III) (Ir(2-phq)₃), the E_T of the host material has to be larger than 2.13 eV.¹⁴ We estimated the E_T of **CzPATPE** by time-gated low temperature emission spectroscopy.⁸ As shown in Fig. 5, the E_T of **CzPATPE** neat thin film was estimated to be 2.05~2.16 eV, which is barely enough for Ir(2-phq)₃ phosphorescent dopant. A clear non-obscure phosphorescence spectrum of the neat film sample is difficult to acquire due to the intense and broad delayed fluorescence spectrum of **CzPATPE**. The HOMO energy level of **CzPATPE** was investigated by a low-energy photoelectron spectrometer (Riken-Keiki AC-2). The optical gap energy estimated from the absorption onset wavelength (401 nm) was used in the calculation of LUMO energy level of the material. As shown in Fig. 6, the HOMO and LUMO energy levels of the **CzPATPE** are 5.93 eV and 2.84 eV, respectively.

Fig. 5 Varied time-gated (top) and varied temperature (bottom) emission spectra of **CzPATPE** neat film.

Fig. 6 Molecular structures of organic materials and their corresponding energy levels alignment.

Based on the same method, we estimated the HOMO and LUMO energy levels of Ir(2-phq)₃ to be 5.24 and 3.08 eV, respectively. The HOMO and LUMO energy levels of TmPyPB (1,3,5-tri(m-pyrid-3-yl-phenyl)benzene) have been reported in literature and they are 6.68 and 2.78 eV, respectively.¹⁵ In order to enhance the EL efficiency of **CzPATPE**:Ir(2-phq)₃ hybrid WOLEDs, a thin film of TmPyPB was fabricated into the device as an electron transporting layer (ETL) or triplet exciton confinement layer (E_T of TmPyPB ~ 2.78 eV)¹⁶ by vacuum thermal deposition after a solution processed **CzPATPE**:Ir(2-phq)₃ white light-emitting layer by spin-coating method (see below).

Having **CzPATPE** as the solution processed host material, a hybrid WOLED was fabricated with a configuration of ITO/PEDOT:PSS (65 nm)/CzPATPE:Ir(2-phq)₃ (99.9:0.1, ~40 nm)/TmPyPB (50 nm)/CsF (2 nm)/Al (100 nm), where PEDOT:PSS (poly(3,4-ethylenedioxythiophene)-poly(styrenesulfonate)) is a solution processed hole-transporting layer of the device. Fig. 7 shows the EL characteristics of **CzPATPE** hybrid WOLED and Table 1 summarizes the corresponding data. Considering two-colour white device and the single phosphorescence dopant Ir(2-phq)₃ which is not a long-wavelength red emitter, a CRI of 72 of the hybrid WOLED is in fact relatively high. This can be mainly attributed to the broad emission band of **CzPATPE** (see Fig. 4b), a typical feature for TPE-based AIE fluorophores.⁷

Fig. 7 (a) EL spectra of the device was recorded at ~60 nits. (b) Voltage dependent current density (mA/cm²) and brightness (cd/m²). (c) Current density dependent current efficiency (cd/A) and power efficiency (lm/W).

Table 1. EL characteristics of **CzPATPE** hybrid WOLED.^a

ETL	Ir(2-phq) ₃ (wt%)	V _{on} (V)	η _{c,max} (cd/A)	η _{p,max} (lm/W)	CIE (x,y)	CRI
TmPyPB	0.1%	5.2	3.4	1.8	(0.36, 0.43)	72

^aV_{on} = turn-on voltage of 10 cd/m²; η_{c,max} and η_{p,max} are maximum current and power efficiencies, respectively.

Conclusions

In summary, a new AIE material **CzPATPE** has been designed and synthesized. We have experimentally demonstrated that **CzPATPE** is thermally stable and readily forms uniform thin film from solution process. It exhibits sky blue fluorescence with reasonable φ_f ~ 40% and large FWHM ~95 nm. Using **CzPATPE** as a fluorescence sky blue emitter as well as the host material for an orange phosphorescence dopant, a hybrid two-colour WOLED with unusually high CRI (> 70) has been successfully demonstrated for the first time. Nevertheless, due to insufficient triplet energy gap of **CzPATPE** for the orange phosphorescence dopant, EL efficiency of such hybrid WOLEDs is not satisfactory. Improved EL efficiency can be achieved with either red phosphorescence dopant having longer emission wavelength (lower triplet energy gap) or further optimization of device structure, which will be reported in due course.

Experimental section

General information

¹H and ¹³C NMR spectra were recorded on a Bruker AV-400 MHz Fourier transform spectrometer at room temperature. Elemental analyses (on a Perkin-Elmer 2400 CHN elemental analyser), matrix-assisted laser desorption/ionization time-of-flight (MALDI-TOF) mass spectroscopy (MS) were performed by the Elemental Analyses and Mass Spectroscopic Laboratory, respectively, in-house service of the Institute of Chemistry, Academic Sinica. Thermal decomposition temperatures (T_d's) of the materials were measured by thermogravimetric analysis (TGA) using Perkin-Elmer TGA-7

analyser systems. Melting temperatures (T_m's) and glass transition temperatures (T_g's) of the materials were measured by differential scanning calorimetry (DSC) using Perkin-Elmer DSC-7 analyser systems. The x-ray diffraction measurement of solution-casting thin film was carried out by using a Bruker D8 Advance diffractometer equipped with a Lynxeye detector. The radiation used was a monochromatic Cu Kα beam of wavelength λ = 0.154 nm. UV-visible absorption spectra were recorded on a Hewlett-Packard 8453 diode array spectrophotometer. Room temperature fluorescence spectra were recorded on a Hitachi fluorescence spectrophotometer F-4500. The ionization potentials (or HOMO energy levels) of the host materials were determined by low energy photo-electron spectrometer (Riken-Keiki AC-2). To measure the triplet energy gap of a thin film sample, we established a system with a temperature control of Model 350 (LakeShore Company) as low as 10 K by Model 22C/350C Cryodyne Refrigerators (Janis Research Company) and a tuneable laser with excitation wavelengths of 213, 266, 355, 532, and 1064 nm (Brilliant B laser, Quantel Company), which is couple to a time-delay controller of LP920 flash photolysis spectrometer (Edinburgh Instrument). The quantum yields of the host material was determined by the integrating-sphere method described by Mello et al. on vacuum-deposited thin film.¹⁷ A He-Cd laser beam (325 or 442 nm) interacts with a solid sample located inside an integrating sphere with an internal diffuse white reflectance coating. The uniformly scattered radiation is coupled to a fused-silica fibre through a baffle-blocked opening, and is detected by a spectrally calibrated spectrometer-CCD (CCD: charge-coupled device) system.

OLED device fabrication and measurements

The ITO substrate was purchased from Buwon with sheet resistance around 25 Ω/sq and thickness of 100 nm. The hole transport layer, poly(3,4-ethylenedioxythiophene) (PEDOT) doped with poly(styrenesulfonate) (PSS) (CH8000), was purchased from Sigma-Aldrich. The TmPyPB electron transport layer and Ir(2-phq)₃ phosphorescent dopant were obtained commercially from either Sigma-Aldrich or Lumtec. The indium tin oxide (ITO) substrates were pre-coated with the PEDOT:PSS hole transporting layer (HTL) and baked in the air at 150 °C for 10 min. Blends of **CzPATPE** and Ir(2-phq)₃ in chlorobenzene were spin-coated on ITO/PEDOT:PSS. The active layer was then annealed at 90 °C for 30 min. After spin-coating active single-layer, the TmPyPB (50 nm), an ultrathin CsF (2 nm) interfacial layer and then aluminium cathode (100 nm) were vacuum-thermal deposited. A surface profiler (Dektak 150 Veeco) was used for calibrating the thickness of HTL and active layer. After the deposition of cathode, the devices were hermetically sealed with glass and UV-cured resins in a glove box (O₂ and H₂O concentration below 0.1 ppm). The device active area was 0.04 cm² was defined by self-made shadow mask applied in the cathode deposition. Current density and voltage characteristics were measured by a dc current/voltage source meter (Keithley 2400), and the device brightness (or electroluminescence, cd/m²), EL spectra, corresponding 1931 CIE_{x,y} chromaticity and colour rendering index (CRI) were monitored and recorded with a spectrophotometer (PR670; Photo Research).

Synthesis

All chemicals were purchased from Aldrich, Alfa Aesar, Acros, and TCI Chemical Co., and they were used without further purifications. Solvents such as dichloromethane (CH₂Cl₂), chlorobenzene, tetrahydrofuran (THF), *N,N*-dimethylformamide (DMF) and xylene and were distilled after drying with appropriate drying agents. The dried solvents were stored over 4 Å molecular sieves before usage. TPENH₂ was obtained from a cross McMurry reaction between benzophenone and 4-aminobenzophenone with ~80% of isolation yields.¹⁰ BrmCP was synthesized from sodium carbazol-9-ide and 1-bromo-2,4-difluorobenzene in ~65% of isolation yields.¹¹

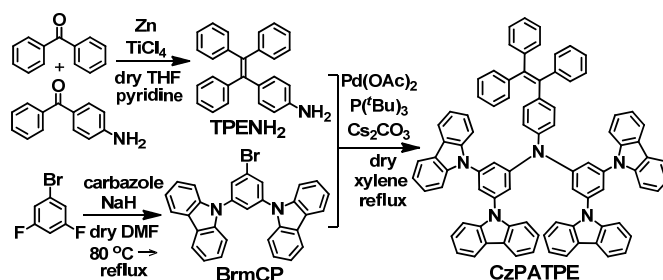
3,5-Di(9H-carbazol-9-yl)-N-(3,5-di(9H-carbazol-9-yl)-phenyl)-N-(4-(1,2,2-triphenylvinyl)phenyl) aniline (CzPATPE). Under dry nitrogen atmosphere, a mixture of BrmCP (5.9 g, 12.1 mmol), TPENH₂ (2.0 g, 5.8 mmol), cesium carbonate (4.5 g, 13.9 mmol), palladium acetate (0.06 g, 0.29 mmol), P(^tBu)₃ (0.28 mL, 1.16 mmol), and dry xylenes (20 mL) was heated at 120 °C for 20 hours. The reaction was quenched by an excess amount of saturated sodium chloride solution. The solution was extracted with dichloromethane. The organic solution was dried over anhydrous MgSO₄. After the removal of drying agent, the solution was evaporated till dryness. The product was subjected to purification by flash column chromatography (silica gel, dichloromethane/hexanes: 1/1). Yield: 52% (3.5 g). ¹H NMR (400 MHz, CDCl₃): δ [ppm] 8.10 (d, *J* = 7.6 Hz, 8H), 7.46-7.41 (m, 14H), 7.26-7.17 (m, 18H), 7.11-7.04 (m, 10H), 6.99-6.96 (m, 2H), 6.82-6.80 (m, 2H), 6.33-6.31 (m, 3H). ¹³C NMR (100 MHz, CDCl₃): δ [ppm] 149.80, 144.62, 143.51, 143.48, 143.20, 142.02, 140.49, 140.46, 140.33, 140.20, 133.35, 131.51, 131.33, 128.57, 128.06, 127.88, 127.56, 126.84, 126.81, 126.72, 126.64, 126.44, 125.97, 124.10, 123.89, 121.11, 120.77, 120.66, 120.63, 119.79, 119.13, 109.98, 109.61. HR-MALDI-TOF-MS: calcd MW, 1159.4614, *m/e* = 1159.4608 (M). Anal. Found (calcd) for C₈₆H₅₇N₅: C 89.12 (89.01), H 5.01 (4.95), N 6.01 (6.04).

Acknowledgements

We thank the Ministry of Science and Technology (MOST 103-2113-M-001-021-MY3), National Taiwan University, and Academia Sinica for financial support.

References

- (a) B. W. D'Andrade, R. J. Holmes, S. R. Forrest, *Adv. Mater.* 2004, **16**, 624. (b) S. Reineke, F. Lindner, G. Schwartz, N. Seidler, K. Walzer, B. Lüssem, K. Leo, *Nature*, 2009, **459**, 234. (c) Q. Wang, J. Ding, D. Ma, Y. Cheng, L. Wang, F. Wang, *Adv. Mater.* 2009, **21**, 2397. (d) H. Sasabe, J.-i. Takamatsu, T. Motoyama, S. Watanabe, G. Wagenblast, N. Langer, O. Molt, E. Fuchs, C. Lennartz, J. Kido, *Adv. Mater.* 2010, **22**, 5003. (e) C.-H. Chang, K.-C. Tien, C.-C. Chen, M.-S. Lin, H.-C. Cheng, S.-H. Liu, C.-C. Wu, J.-Y. Hung, Y.-C. Chiu, Y. Chi, *Org. Electron.* 2010, **11**, 412.
- (a) C.-L. Ho, W.-Y. Wong, Q. Wang, D. Ma, L. Wang, Z. Lin, *Adv. Funct. Mater.* 2008, **18**, 928. (b) W.-Y. Hung, L.-C. Chi, W.-J. Chen, Y.-M. Chen, S.-H. Chou and K.-T. Wong, *J. Mater. Chem.*, 2010, **20**, 10113. (c) T. Zhang, M. Liu, T. Li, J. Ma, D. Liu, W. Xie, C.-L. Wu, S.-W. Liu, S.-C. Yeh, C.-T. Chen, *J. Phys. Chem. C*, 2011, **115**, 2428. (d) S. Hofmann, M. Furno, B. Lüssem, K. Leo and M. C. Gather, *Phys. Status Solidi A*, 2013, **210**, 1467. (e) J. Wan, C.-J. Zheng, M.-K. Fung, X.-K. Liu, C.-S. Lee and X.-H. Zhang, *J. Mater. Chem.*, 2012, **22**, 4502. (f) J. Ye, C.-J. Zheng, X.-M. Ou, X.-H. Zhang, M.-K. Fung and C.-S. Lee, *Adv. Mater.*, 2012, **24**, 3410.
- (a) L. Duan, L. Hou, T.-W. Lee, J. Qiao, D. Zhang, G. Dong, L. Wang and Y. Qiu, *J. Mater. Chem.* 2010, **20**, 6392. (b) C. Zhong, C. Duan, F. Huang, H. Wu and Y. Cao, *Chem. Mater.* 2011, **23**, 326.
- M.-F. Wu, S.-J. Yeh, C.-T. Chen, H. Murayama, T. Tsuboi, W.-S. Li, I. Chao, S.-W. Liu and J.-K. Wang, *Adv. Funct. Mater.* 2007, **17**, 1887.
- T. Haskins, A. Chowdhury, R. H. Young, J. R. Lenhard, A. P. Marchetti and L. J. Rothberg, *Chem. Mater.*, 2004, **16**, 4675.
- (a) J. Luo, Z. Xie, J. W. Y. Lam, L. Cheng, H. Chen, C. Qiu, H. S. Kwok, X. Zhan, Y. Liu, D. Zhu and B. Z. Tang, *Chem. Commun.*, 2001, 1740. (b) Y. Hong, J. W. Y. Lam, B. Z. Tang, *Chem Soc. Rev.* 2011, **40**, 5361.
- (a) Z. Zhao, J. W. Y. Lam, B. Z. Tang, *J. Mater. Chem.* 2012, **22**, 23726. (b) J. Huang, X. Yang, X. Li, P. Chen, R. Tang, F. Li, P. Lu, Y. Ma, L. Wang, J. Qin, Q. Li and Z. Li, *Chem. Commun.*, 2012, **48**, 9586. (c) Z. Chang, Y. Jiang, B. He, J. Chen, Z. Yang, P. Lu, H. S. Kwok, Z. Zhao, H. Qiu and B. Z. Tang, *Chem. Commun.*, 2013, 49, 594. (d) J. Huang, N. Sun, P. Chen, R. Tang, Q. Li, D. Ma and Z. Li, *Chem. Commun.*, 2014, **50**, 2136. (e) X. Y. Shen, Y. J. Wang, E. Zhao, W. Z. Yuan, Y. Liu, P. Lu, A. Qin, Y. Ma, J. Z. Sun and B. Z. Tang, *J. Phys. Chem. C*, 2013, **117**, 7334. (f) J. Huang, N. Sun, Y. Dong, R. Tang, P. Lu, P. Cai, Q. Li, D. Ma, J. Qin, Z. Li, *Adv. Funct. Mater.* 2013, **23**, 2329. (g) J. Huang, Y. Jiang, R. Tang, N. Xie, Q. Li, H. S. Kwok, B. Z. Tang, Z. Li, *J. Mater. Chem. C*, 2014, **2**, 2028.
- Y.-T. Lee, Y.-T. Chang, M.-T. Lee, P.-H. Chiang, C.-T. Chen and C.-T. Chen, *J. Mater. Chem. C*, 2014, **2**, 382.
- X. Zhan, Z. Wu, Y. Lin, Y. Xie, Q. Peng, Q. Li, D. Ma and Z. Li, *Chem. Sci.* 2016, **7**, DOI: 10.1039/c6sc00559d.
- X.-F. Duan, J. Zeng, J.-W. Lü and Z.-B. Zhang, *J. Org. Chem.*, 2006, **71**, 9873.
- M. Yabe, T. Shioya, H. Sato, S. Akiyama, JP Patent 2005047811 A.
- (a) W. Z. Yuan, P. Lu, S. Chen, J. W. Y. Lam, Z. Wang, Y. Liu, H. S. Kwok, Y. Ma and B. Z. Tang, *Adv. Mater.* 2010, **22**, 2159. (b) Z. Zhao, S. Chen, J. W. Y. Lam, C. Y. K. Chan, C. K. W. Jim, Z. Wang, C. Wang, P. Lu, H. S. Kwok, Y. Ma and B. Z. Tang, *Pure Appl. Chem.* 2010, **82**, 863. (c) Y. Liu, S. Chen, J. W. Y. Lam, P. Lu, R. T. K. Kwok, F. Mahtab, H. S. Kwok and B. Z. Tang, *Chem. Mater.* 2011, **23**, 2536.
- C.-L. Chiang, M.-F. Wu, D.-C. Dai, Y.-S. Wen, J.-K. Wang and C.-T. Chen, *Adv. Funct. Mater.*, 2005, **15**, 231.
- A. Endo and C. Adachi, *Chem. Phys. Lett.*, 2009, **483**, 224.
- S.-J. Yoo, H.-J. Yun, I. Kang, K. Thangaraju, S.-K. Kwon, Y.-H. Kim, *J. Mater. Chem. C*, **2013**, **1**, 2217.
- C. Fan, L. Zhu, T. Liu, B. Jiang, D. Ma, J. Qin, C. Yang, *Angew. Chem. Int. Ed.* **2014**, **126**, 2179.
- J. C. de Mello, H. F. Wittmann, R. H. Friend, *Adv. Mater.* 1997, **9**, 230.



Scheme 1 Synthesis of CzPATPE.

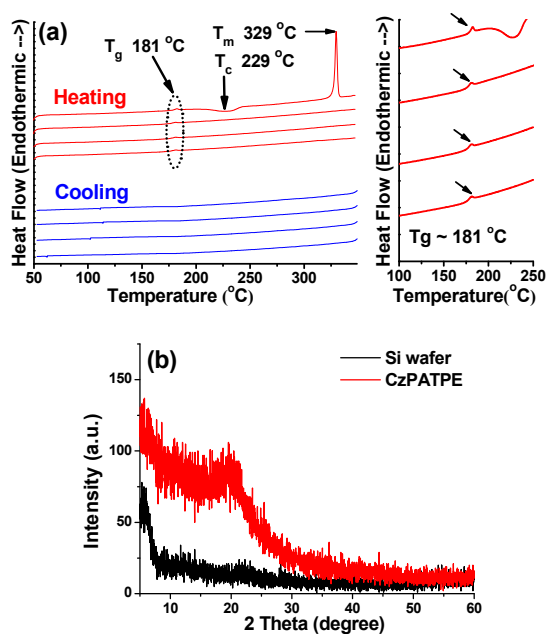


Fig. 1 (a) DSC thermograms. (b) X-ray diffraction spectra of CzPATPE thin film on a substrate of silicon wafer.

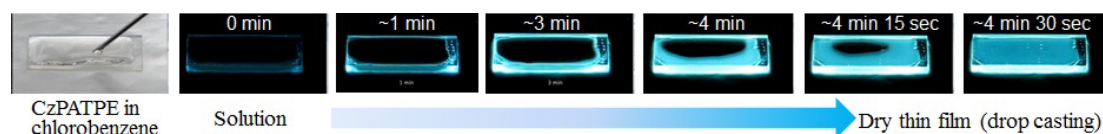


Fig. 2 CzPATPE drop-casting solution under visible light (far left) and under UV illumination during the solvent evaporation at ~ 90 °C (the rest of six photographs).

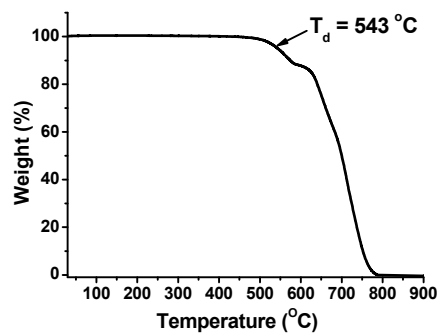


Fig. 3 TGA thermogram of CzPATPE.

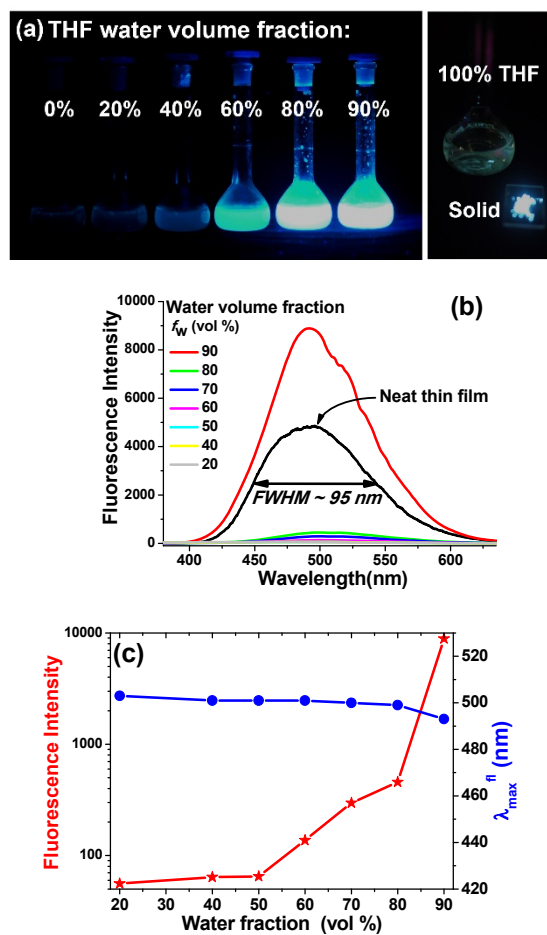


Fig. 4 CzPATPE THF solution with various water volume fraction (f_w): (a) Fluorescence image. (b) Fluorescence spectra (c) Variation of fluorescence intensity and fluorescence wavelength ($\lambda_{\max}^{\text{fl}}$).

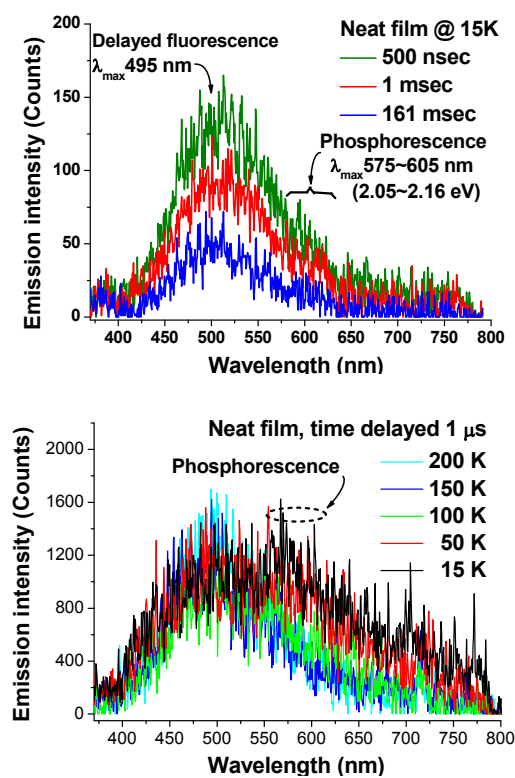


Fig. 5 Varied time-gated (top) and varied temperature (bottom) emission spectra of CzPATPE neat film.

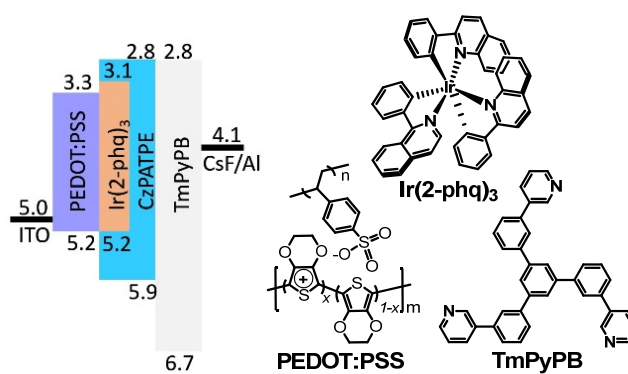


Fig. 6 Molecular structures of organic materials and their corresponding energy levels alignment.

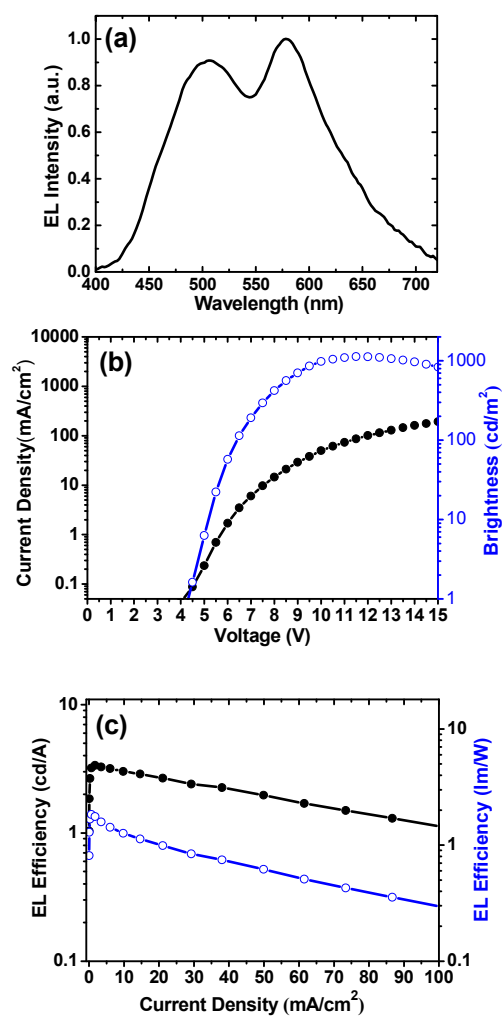
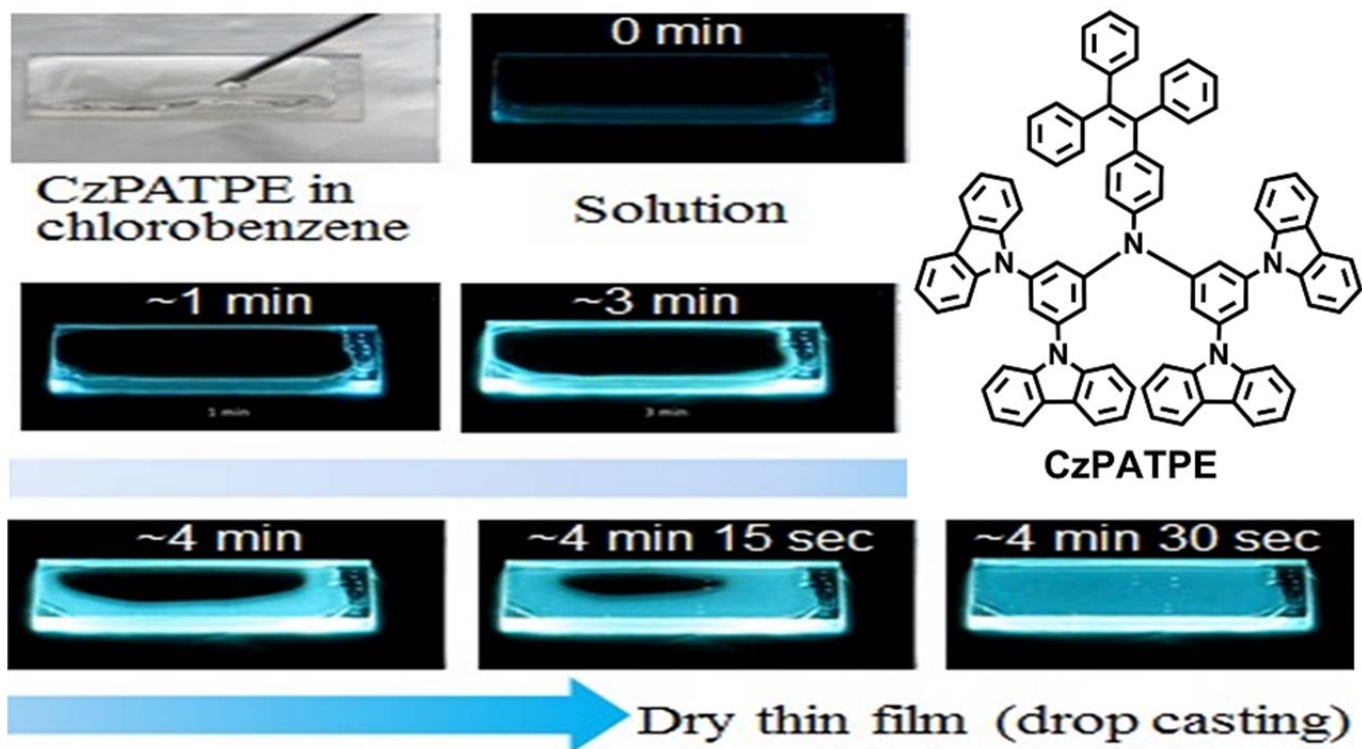


Fig. 7 (a) EL spectra of the device was recorded at ~ 60 nits. (b) Voltage dependent current density (mA/cm^2) and brightness (cd/m^2). (c) Current density dependent current efficiency (cd/A) and power efficiency (lm/W).



CzPATPE AIE fluorophore for solution processed host material in hybrid white OLEDs.